Journal of Magnetism and Magnetic Materials 375 (2015) 153–163

Contents lists available at ScienceDirect

Journal of Magnetism and Magnetic Materials

journal homepage: www.elsevier.com/locate/jmmm

Local magnetic properties of multiferroic $Nd_{0.5}Gd_{0.5}Fe_3(BO_3)_4$ in the excited states of Nd^{3+} ion

A.V. Malakhovskii [a,*], S.L. Gnatchenko [b], I.S. Kachur [b], V.G. Piryatinskaya [b], A.L. Sukhachev [a], V.L. Temerov [a]

[a] L. V. Kirensky Institute of Physics, Siberian Branch of Russian Academy of Sciences, 660036 Krasnoyarsk, Russian Federation
[b] B. Verkin Institute for Low Temperature Physics and Engineering, National Academy of Sciences of Ukraine, 61103 Kharkov, Ukraine

ARTICLE INFO

Article history:
Received 11 August 2014
Received in revised form
24 September 2014
Accepted 24 September 2014
Available online 12 October 2014

Keywords:
f-f transitions
Nd^{3+} ion
Excited states
Local magnetic properties

ABSTRACT

Polarized absorption spectra of single-crystal $Nd_{0.5}Gd_{0.5}Fe_3(BO_3)_4$ were studied in the region of the transition $^4I_{9/2} \rightarrow (^4G_{5/2} + {}^2G_{7/2})$ in Nd^{3+} ion as a function of temperature (2–34 K) and magnetic field (0–65 kOe). The spectra of natural circular dichroism were measured in the range of 5–40 K. It was found out that the local magnetic properties in the vicinity of the excited ion substantially depended on its state. In particular, a weak ferromagnetic moment appears in some excited states. It was found out that the selection rules for electron transitions in the magnetically ordered state substantially deviated from those in the paramagnetic state of the crystal. They are different for different transitions and they are very sensitive to the orientation of the sublattice magnetic moment relative to the light polarization. In the spectrum of the natural circular dichroism, the transition is revealed which is not observed in the absorption spectrum.

1. Introduction

An electronically excited atom is, actually, an impurity atom, and, consequently, the local properties of a crystal in the vicinity of the excited atom can change. Spectroscopic manifestations of such local alterations connected with electronic transitions were observed in $RbMnF_3$ and MnF_2, [1] in $FeBO_3$ [2] and in some rare earth (RE) containing crystals of huntite structure [3–6]. In Ref. [7] it was shown that during the electron transition the initial state of the ion and its interaction with the environment also changed and could have an influence upon the polarization of transitions. If there are many excited atoms, not only the local properties can change. So, in Ref. [8] a phase transition under the influence of the powerful laser pulse was described.

The present work is devoted to the study of two main phenomena: 1) the influence of the magnetic ordering on the *f-f* electron transitions properties (selection rules, in particular); 2) the change of the local magnetic and symmetry properties in the excited 4*f* states. The investigation of the local properties of crystals in the optically excited states has become important in recent years in connection with the problem of the quantum information processing (see e. g., Refs. [9–12]). Crystals containing RE ions are widely used in these efforts. For example, a change of the local crystal properties near the optically excited atom was used for reading out the information in the quantum memory [10].

The family of RE ferroborates with the common chemical formula $RFe_3(BO_3)_4$ has been widely investigated during the last years. The fundamental interest to these compounds is conditioned by the coexistence and mutual influence of two magnetic subsystems: iron and RE ones which results in a large variety of magnetic properties of the crystals. All RE ferroborates are ordered antiferromagnetically at temperatures below 30–40 K. Depending on the choice of a RE ion, they can have an easy-axis or easy-plane magnetic structure. The variation of temperature and external magnetic field leads to various kinds of phase transitions, including spin-reorientation and commensurate-to-incommensurate ones. Some crystals also exhibit structural phase transitions. Additionally, it has recently been found that many of RE ferroborates demonstrate a considerable coupling between the magnetic ordering and electric polarization [13–17]. This allows one to refer these compounds to the class of multiferroics. The investigation of multiferroic materials is of great interest now, both in the fundamental aspect (clarifying the mechanism of the magnetoelectric coupling) and in view of their potential technological applications.

The $Nd_{0.5}Gd_{0.5}Fe_3(BO_3)_4$ crystal, the same as the pure Nd and Gd-ferroborates, reveals multiferroic properties [18]. It is an easy plane antiferromagnet from $T_N = 32$ K down to at least 2 K [19]. For

* Corresponding author. Fax: 7 391 2438923.
E-mail address: malakha@iph.krasn.ru (A.V. Malakhovskii).

http://dx.doi.org/10.1016/j.jmmm.2014.09.077
0304-8853/

future discussion it is important that at temperatures $T<11$ K a hysteresis in the magnetization of the crystal in the easy plane was found, indicating appearance of the static magnetic domains [19]. The crystal has trigonal symmetry with the space group $R32$ and the lattice constants are: $a=9.557(7)$ Å and $c=7.62(1)$ Å [19]. Trivalent RE ions occupy D_3 symmetry positions. They are located at the center of trigonal prisms made up of six crystallography equivalent oxygen ions. All Fe ions occupy C_2-symmetry positions. Structural phase transitions were not found down to 2 K [19]. The magnetic structure of the $Nd_{0.5}Gd_{0.5}Fe_3(BO_3)_4$ crystal was not studied in detail. However, its magnetic properties [19] are close to those of the related crystal $NdFe_3(BO_3)_4$ [20–23]. Therefore, it is possible to suppose that the magnetic structure of these crystals is also similar. In particular, neutron diffraction measurements of $NdFe_3(^{11}BO_3)_4$ testified to magnetic spiral configurations with the magnetic moments oriented parallel to the hexagonal basal plane [24]. Later [25] it was shown that in the commensurate magnetic phase below $T_N\approx 30$ K all three magnetic Fe moments and the magnetic Nd moment were aligned ferromagnetically in the basal hexagonal plane but aligned antiferromagnetically between the adjacent planes. It was also shown that in the incommensurate spiral magnetic phase (below $T\approx 13.5$ K) the magnetic structure of $NdFe_3(^{11}BO_3)_4$ was transformed into a long-period antiferromagnetic helix with single chirality. In Ref. [26] it was shown that this phase transition behaved as the first order one. Nonresonant x-ray magnetic scattering showed that the correlation length (or size) of the magnetic domains was around 100 Å [27]. An element selective resonant magnetic x-ray scattering study has confirmed that the magnetic order of the Nd sublattice is induced by the Fe spin order [28]. When the magnetic field is applied parallel to the hexagonal basal plane, the helicoidal spin order is suppressed and a collinear ordering, where the moments are forced to align in the direction perpendicular to the applied magnetic field, is stabilized [28].

The absorption spectra of $Nd_{0.5}Gd_{0.5}Fe_3(BO_3)_4$ single crystal had been earlier analyzed with the help of the Judd-Ofelt theory and spectroscopic characteristics of the crystal had been obtained [29]. The optical and magneto-optical properties of the $Nd_{0.5}Gd_{0.5}Fe_3(BO_3)_4$ crystal in the near IR spectral region were studied in Ref. [30]. Optical spectra and crystal field parameters of the related crystal $NdFe_3(BO_3)_4$ were studied in Ref. [23].

2. Experimental details

$Nd_{0.5}Gd_{0.5}Fe_3(BO_3)_4$ single crystals were grown from the melt solution on the basis of $K_2Mo_3O_{10}$ as described in Ref. [31]. The sample used for optical absorption measurements was a 0.2 mm-thick plane-parallel polished plate oriented parallel to the crystallographic axis C_3. Absorption spectra were measured using a diffraction monochromator MDR-23 with the diffraction grating 1200 lines/mm and linear dispersion 1.3 nm/mm. The spectral resolution was about 1.5 cm^{-1} in the studied spectral region. The light intensity was measured by a photomultiplier with further computer registration. The absorption spectra were measured with the light propagating normal to the C_3 axis of the crystal, electric vector of light being parallel (the π-spectrum) or perpendicular (the σ-spectrum) to the C_3 axis. The light was polarized by the Glan prism.

Natural circular dichroism (NCD) spectra were studied on the sample of 0.215 mm-thick cut perpendicular to the C_3 axis of the crystal and with light propagated parallel to C_3 axis (α-polarization). The NCD spectra were measured by the method of light-polarization modulation using a piezoelectric modulator (details see in Ref. [32]). Spectral resolution at NCD measurements was about 2.3 cm^{-1}.

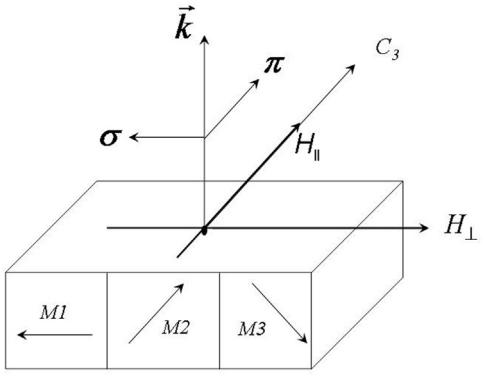

Fig. 1. Geometry of experiments.

Magnetic field was created by a superconducting solenoid with Helmholtz type coils. The magnetic field direction was parallel to the surface of the sample and perpendicular or parallel to the C_3 axis (Fig. 1). The superconducting solenoid with the sample was placed in liquid helium and all measurements in the magnetic field were fulfilled at $T=2$ K. For the temperature measurements of absorption and natural circular dichroism spectra a liquid-helium cooled cryostat was used. It had an internal volume filled by gaseous helium where the sample was placed. The temperature of the sample was regulated by a heating element.

3. Results and discussion

3.1. Identification of excited states

Polarized absorption spectra of the $Nd_{0.5}Gd_{0.5}Fe_3(BO_3)_4$ single crystal in the region of the transition $^4I_{9/2}\rightarrow(^4G_{5/2}+^2G_{7/2})$ at $T=6$ K and at $T=33$ K (above T_N) are shown in Figs. 2a and 2b respectively. Symmetry of the ground state $Gr1$ of Nd^{3+} ion in the crystal was identified earlier [30] (see Table 1). The excited state of the D-manifold ($^4G_{5/2}+^2G_{7/2}$) is split in the crystal field of D_3 symmetry in the following way: $^4G_{5/2}$: $2E_{1/2}+E_{3/2}$ and $^2G_{7/2}$: $3E_{1/2}+E_{3/2}$. The symmetries of the states in the D-manifold are found (Table 1) according to the linear polarizations of the absorption lines (Figs. 2a, 2b and Table 1), selection rules of Table 2 and symmetry of the ground state. The polarization of $D1(Gr2)$ and $D2(Gr2)$ transitions (Fig. 2b) from the first excited state $Gr2$ of the ground manifold gives symmetry of this state (Table 1). Shape of $D1(Gr2)$ and $D2(Gr2)$ lines is apparently due to the phonon side-bands caused by acoustic phonons.

In a trigonal crystal, for half integer total moment there are three possible values of the crystal quantum number [33]: $\mu=+1/2$, -1/2, 3/2 ($\pm 3/2$). States with $M_J=\mu\pm 3n$ (where $n=0, 1, 2, \ldots$) correspond to each μ in the trigonal symmetry [33]. As a result, the following set of states is obtained:

$$M_J=\pm 1/2, \pm 3/2, \pm 5/2, \pm 7/2, \pm 9/2;$$
$$\mu=\pm 1/2, (\pm 3/2), \mp 1/2, \pm 1/2, (\pm 3/2) \quad (1)$$

The set of the crystal field states for J-multiplets of Nd^{3+} ion is evidently found according to value of J. The states with $\mu=\pm 1/2$ correspond to the states $E_{1/2}$ and the states with $\mu=(\pm 3/2)$ correspond to the states $E_{3/2}$ in the D_3 group notations.

The electron states of a free atom in a homogeneous electric field ($C_{\infty v}$ symmetry) are split according to the absolute value of the magnetic quantum number M_J. The electron states of an atom in the trigonal crystal field are also split according to the absolute values of M_J, in the first approximation. Therefore, the atom wave functions can be described by $|J, \pm M_J\rangle$ states. In this

approximation, the effective Landé factor of the Kramers duplets along C_3 axis is defined by the equation [7]:

$$g_{CM} = 2gM_J \quad (2)$$

where g is the Landé factor of the free atom. The results for Nd^{3+} ion are shown in Table 3. The states with the same μ and different M_J (see Eq. 1) can mix in the crystal, and resulting g_C can be both smaller and larger than g_{CM}. The prevailing M_J states of the free atom in the crystal field states of the D-manifold (Table 1) can be found based on the comparison of g_{CM} for the corresponding M_J (Tables 3 and 1) with the theoretical g_C in the $NdFe_3(BO_3)_4$ crystal (Table 1). They are of course different but the succession of values permits to identify origin of D-states from the M_J states (see Table 1).

The presented selection rules and identifications refer to paramagnetic state of the crystal. The magnetic ordering introduces substantial changes in the situation.

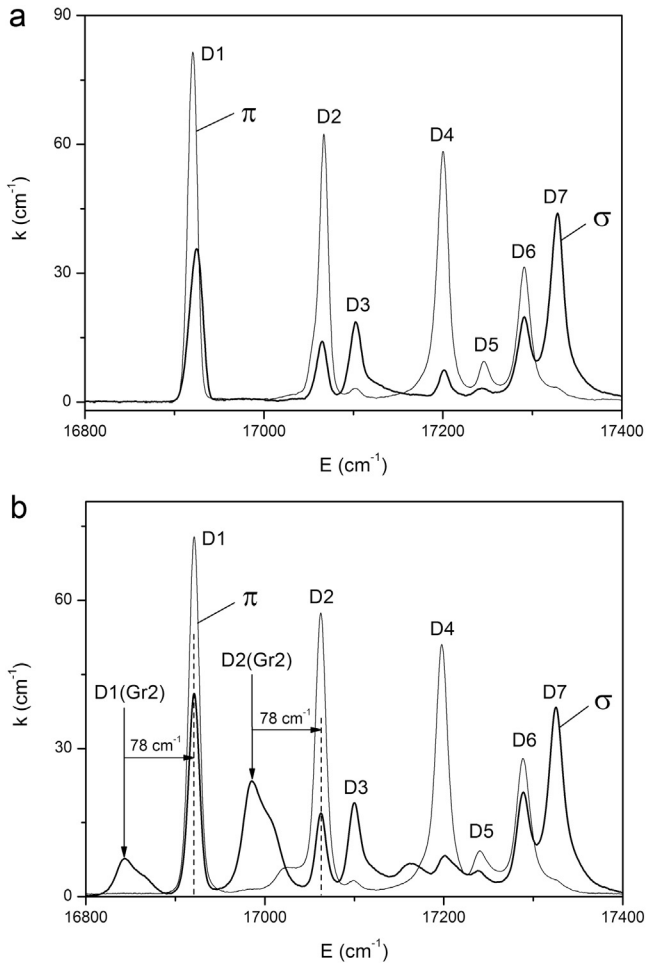

Fig. 2. (a). Polarized absorption spectra of $^4I_{9/2} \rightarrow (^4G_{5/2} + {}^2G_{7/2})$ transition (D-band) at 6 K. (b). Polarized absorption spectra of $^4I_{9/2} \rightarrow (^4G_{5/2} + {}^2G_{7/2})$ transition (D-band) at 33 K.

3.2. Behavior of absorption lines as a function of the magnetic field and temperature

3.2.1. D1 line

At temperatures $T < T_N$ electronic states of the Nd^{3+} ion are split by the exchange field of the magnetically ordered Fe-subsystem (Fig. 3). As mentioned above, the measurements in magnetic field were fulfilled at $T=2$ K. At this temperature only transitions from the lower sublevel of the ground state exchange splitting can be observed. (Generally, there are possible four transitions between components of the ground and excited state exchange splitting (Fig. 3)). At the zero magnetic field, $D1\sigma$ line consists of two components of the Gaussian shape: $D1a\sigma$ and $D1c\sigma$ (see Fig. 4), corresponding to the transitions into the components of the excited state exchange splitting (Fig. 3). We supposed that the more intensive component, $D1a\sigma$, corresponds to the transition without overturn of the Nd ion magnetic moment (Fig. 3). Positions of $D1a\sigma$ and $D1c\sigma$ lines as a function of magnetic field directed perpendicular to C_3 axis are shown in Fig. 5. In the same figure there is the field dependence of the $D1\pi$ line position. $D1\pi$ line is not decomposed into components and can be identified as $D1a\pi$ line according to its energy. Thus, $D1c$ line is not active in π-polarization (see Fig. 3). In Fig. 5 (inset) there is the field dependence of the position of the undecomposed $D1\sigma$ line

Table 2
Selection rules for electric dipole transitions in D_3 symmetry.

	$E_{1/2}$	$E_{3/2}$
$E_{1/2}$	π, $\sigma(\alpha)$	$\sigma(\alpha)$
$E_{3/2}$	$\sigma(\alpha)$	π

Table 3
Landé factors of the Kramers doublets along C_3 axis of a crystal in approximation of $|J, \pm M_J\rangle$ states of the free atom.

	M_J	13/2	11/2	9/2	7/2	5/2	3/2	1/2
$^4I_{9/2}$, $g=0.727$	g_{CM}			6.54	5.09	3.64	2.18	0.727
$^4G_{5/2}$, $g=0.571$	g_{CM}					2.855	1.713	0.571
$^2G_{7/2}$, $g=0.889$	g_{CM}				6.223	4.445	2.667	0.889

Table 1
Parameters of transitions and states. $\Delta E1$ – exchange splitting of absorption lines, connected with the exchange splitting of the ground state, $\Delta E2$-exchange splitting of excited states, g_{CM}-values of g_C in approximation of $|J, \pm M_J\rangle$ states of the free atom. Energies of transitions (E) are given at 40 K (above T_N). Details are in the text.

State	Level	E cm^{-1}	Polar.	Sym.	μ	M_J	$\Delta E1$ (π) cm^{-1}	$\Delta E1$ (σ) cm^{-1}	$\Delta E2$ cm^{-1}	$g_\perp$ [23]	g_C [23]	g_{CM}
$^4I_{9/2}$	$Gr1$	0	–	$E_{1/2}$	$\mp 1/2$	$\pm 5/2$				2.385	1.376	3.64
	$Gr2$	~78	–	$E_{3/2}$	3/2	$\pm 9/2$				0	3.947	6.54
$^4G_{5/2}$	$D1$	16921	π, σ	$E_{1/2}$	$\pm 1/2$	$\pm 1/2$			7	0.043	0.065	0.571
	$D2$	17062	π, σ	$E_{1/2}$	$\mp 1/2$	$\pm 5/2$	14.2		2	1.385	1.310	2.885
	$D3$	17100	$\approx\sigma$	$E_{3/2}$	3/2	$\pm 3/2$			0	0	3.044	1.713
$^2G_{7/2}$	$D4$	17199	π, σ	$E_{1/2}$	$\pm 1/2$	$\pm 1/2$			12	2.617	0.266	0.889
	$D5$	17240	π, σ	$E_{1/2}$	$\pm 1/2$	$\pm 7/2$	~17		7.5	0.755	3.308	6.223
	$D6$	17289	π, σ	$E_{1/2}$	$\mp 1/2$	$\pm 5/2$			0.4	1.538	0.954	4.445
	$D7$	17325	$\approx\sigma$	$E_{3/2}$	3/2	$\pm 3/2$			0	0	1.016	2.667

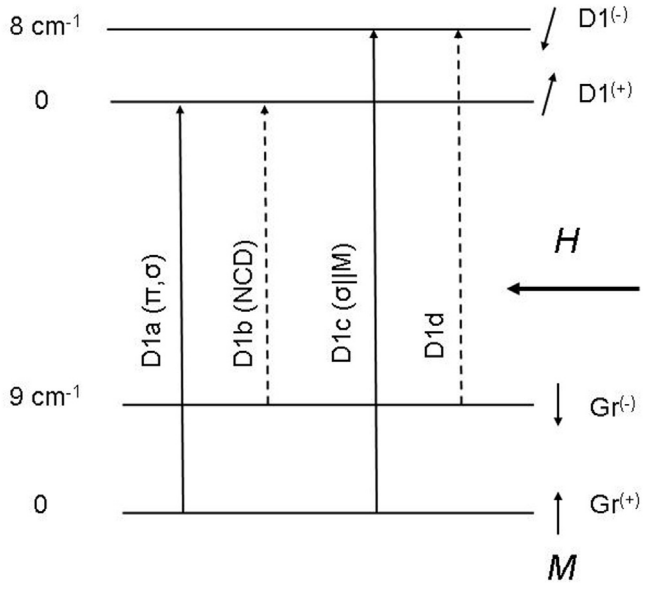

Fig. 3. Diagram of the $D1$ transitions.

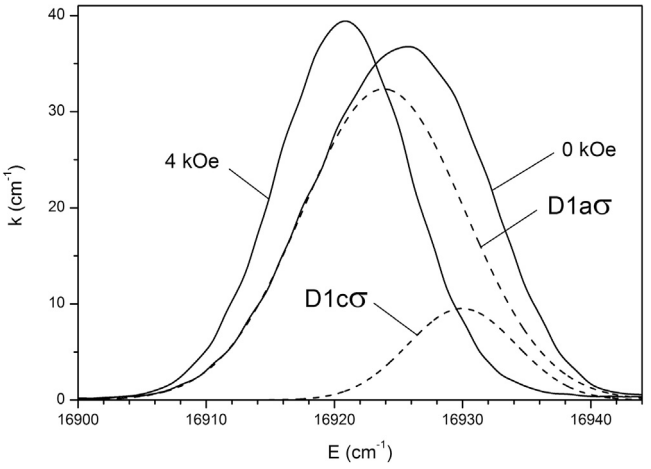

Fig. 4. σ-polarized absorption spectra of $D1$ line at $T=2$ K in magnetic field $H\perp C_3$.

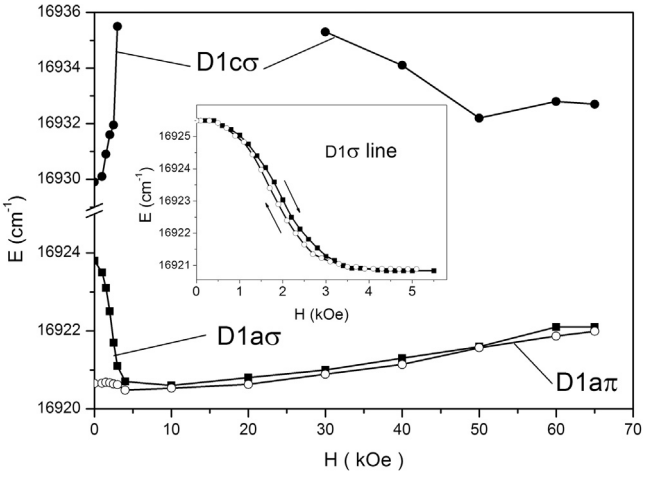

Fig. 5. The $D1$ transitions energies as a function of magnetic field $H\perp C_3$ at $T=2$ K. Inset: position of the undecomposed $D1\sigma$ line maximum.

maximum, which demonstrates hysteresis in the crystal remagnetization [19]. Fig. 6 shows a variation of the lines intensities as a function of the magnetic field perpendicular to C_3 axis. Fig. 6

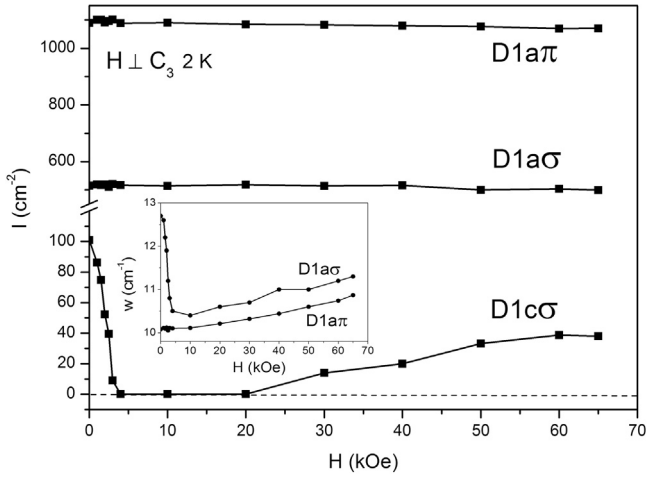

Fig. 6. The $D1$ transitions intensities as a function of magnetic field $H\perp C_3$ at $T=2$ K. Inset: line widths as a function of magnetic field $H\perp C_3$.

demonstrates that in the field $H>4$ kOe the $D1c\sigma$ line disappears. $H=4$ kOe is the spin-flop field and simultaneously the one domain state field in the basal plane [19] (see also Fig. 5, inset). In this case magnetic moments of ions in the whole crystal become oriented perpendicular to the magnetic field and to the σ-polarization (Fig. 1). Thus, $D1c$ line is allowed only in σ-polarization and when $M\|\sigma$ (Fig. 3). At higher fields a component of the magnetic moment $M\|\sigma$ appears and, correspondingly, $D1c\sigma$ line appears again (Fig. 6). Intensity of $D1a\pi$ line practically does not depend on magnetic field (Fig. 6) since always $\pi\perp M$ (Fig. 1). The orientation of the magnetic moments depending on the magnetic field $H\perp C_3$ in the region of 0-4 kOe does not influence the intensity of $D1a\sigma$ line (Fig. 6) but influences its energy (Fig. 5). It is a consequence of different energy of different domains in magnetic field. The energy of $D1a\pi$ line also decreases in the same field region (Fig. 5) but to a smaller degree, i. e., it seems that the energy of the state depends on the transition polarization, or it looks like the splitting of the $D1a$ line that is not possible for the Kramers doublet. Apparently, we deal with two absorbing objects: domains and domain walls with different energies and polarizations of the transitions. Indeed, at $H>4$ kOe, when there are no domain walls, the energies of $D1a\sigma$ and $D1a\pi$ lines coincide. The $D1$ lines are well approximated by Gaussians that testifies to the inhomogeneous nature of the line widths. The $D1a\sigma$ line width decreases in the region of 0-4 kOe (Fig. 6, inset), when the crystal transfers to the one domain state. This corresponds to the transfer of the crystal to a higher magnetic homogeneity. $D1a\pi$ line does not reveal such behavior. This is a consequence of the mentioned above smaller influence of the magnetic state on the $D1a\pi$ transition energy.

After the spin-flop, the energies of both exchange split components of antiferromagnet change identically in the magnetic field due to the sublattice angularity caused by the magnetic field. So, the change of a line frequency, defined by the difference of the ground and excited state energy variations, should be identical for lines $D1a\sigma$ and $D1c\sigma$, corresponding to the transitions into the sublevels of the excited state exchange splitting. This contradicts to Fig. 5. The observed dependences of Fig. 5 can be accounted for in an assumption that a spontaneous sublattice angularity (a weak ferromagnetic moment ΔM) occurs in the excited $D1$ state. This ferromagnetic moment has the opposite direction in $D1^{(+)}$ and $D1^{(-)}$ states (Fig. 3). The energy of this moment in the magnetic field also changes in the opposite directions in the $D1^{(+)}$ and $D1^{(-)}$ states. In the magnetic field parallel to C_3 axis the energies of the

considered absorption lines steadily increase, i. e., the spontaneous sublattice angularity does not occur in this direction.

The transitions $D1b$ and $D1d$ (Fig. 3) from the upper sublevel of the ground state exchange splitting should appear on the lower energy side of the absorption spectrum with the increasing temperature. The ground state exchange splitting at 6 K is $\sim 9\ cm^{-1}$ [30]. Therefore, energy of the $D1b$ transition at 6 K should be $9\ cm^{-1}$ less than that of the $D1a$ transition and so the D1b transition is certainly not observed in the absorption spectra of Fig. 7, inset. Absorption spectra of the $D1$ transition in σ-polarization (Fig. 7, inset) were decomposed into Gaussian components $D1a\sigma$ and $D1c\sigma$ in the temperature range 6-33 K, and the temperature dependences of the positions and intensities of the components were obtained (Figs. 7 and 8). Temperature behavior of energy of the π-polarized $D1a$ line ($D1a\pi$ line) is also shown in Fig. 7. The difference of the $D1a\sigma$ and $D1c\sigma$ line energies at T=6-16 K (Fig. 7) gives the exchange splitting of the excited state of $\sim 8\ cm^{-1}$ (Fig. 3). Energy of the $D1d$ transition is close to that of the $D1a$ transition (Fig. 3), since the exchange splitting of the excited state at 6 K is close to that of the ground state and therefore the $D1d$ transition can take part in the $D1a$ line intensity at increasing temperature. The $D1$ transition in the paramagnetic state of the crystal is active both in π- and σ-polarizations (Table 1). However, in the magnetically ordered state the $D1c$ transition is active only in σ-polarization and only when $M \| \sigma$.

From Fig. 8 it is seen that at $T \sim 20$ K the $D1c\sigma$ line disappears. The observed phenomenon is evidently connected with the exchange interaction in the excited state and has a threshold character. This can be explained by the appearance of the mentioned above weak ferromagnetic moment ΔM in the excited state at $T < 20$ K. It is quite natural that the ferromagnetic moment in the excited state appears at temperature lower than T_N, corresponding to the ground electron state. Figs. 7 and 8 testify that the splitting between $D1a\sigma$ and $D1c\sigma$ lines is defined by the antiferromagnetic exchange interaction, but the intensity of the $D1c\sigma$ line increases with increasing weak ferromagnetic moment ΔM. Thus, it would be more properly to characterize selection rule for $D1c\sigma$ line not relative to sublattice magnetic moment M but relative to ferromagnetic moment: $\sigma \perp \Delta M$.

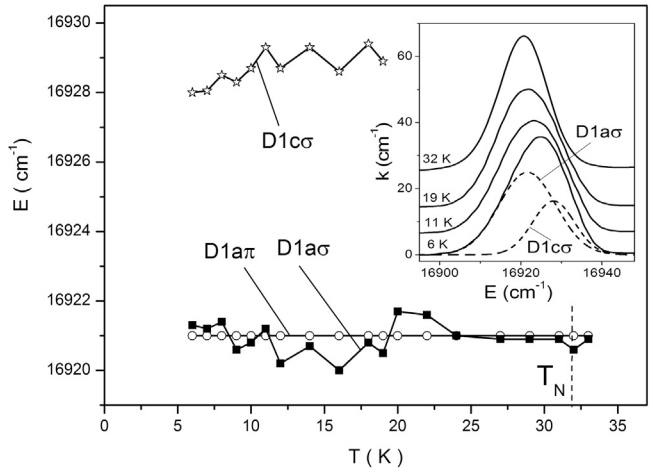

Fig. 7. The $D1$ transitions energies as a function of temperature in zero magnetic field. Inset: σ-polarized absorption lines at several temperatures.

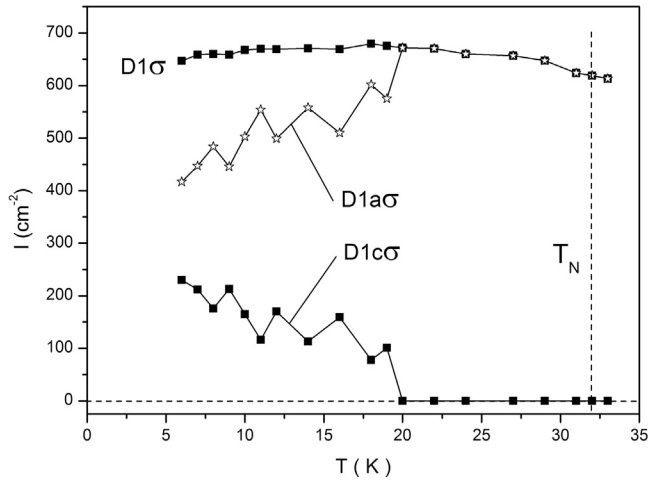

Fig. 8. The $D1$ transitions intensities as a function of temperature in zero magnetic field.

3.2.2. D2 line

Fig. 9 presents π-spectra of the $D2$ line at three temperatures. The spectra of the σ-polarized $D2$ line at three temperatures are shown in Fig. 9, inset. At T=2 K only the transitions from the lower sublevel of the ground state exchange splitting are observed. $D2\pi$ and $D2\sigma$ lines at this temperature are not split (are well approximated by one Gauss function) and have different energies. Therefore, they can be considered as separate transitions to sublevels of the excited state exchange splitting (see the $D2$ transitions diagram in Fig. 10). At the increasing temperature, the $D2b\pi$ line (Fig. 9) corresponding to the transition from the upper sublevel of the ground state exchange splitting appears. The positions of lines $D2a\pi$ and $D2b\pi$ as a function of temperature (Fig. 11) were found as the positions of negative extremums in the second derivatives spectra. The $D2d\sigma$ line (Fig. 9, inset), corresponding to the transition between the upper sublevels of the ground and excited states exchange splitting (Fig. 10), is very weak, and its dependence on temperature can not be found. Position of the $D2c\sigma$ line (Fig. 10) is given in Fig. 11 as the position of the maximum of the total σ-spectrum. At low temperature, when only the lower sublevel of the ground state exchange splitting is occupied, and at a temperature near T_N this curve gives the correct position of the $D2c\sigma$ line. So, the distance between $D2a\pi$ and $D2c\sigma$ lines gives the exchange splitting of the excited state at 6 K equal to $\sim 2\ cm^{-1}$. In the temperature behavior of $D2$ lines (Fig. 11) there are no indications of any features in the region of T=20 K, unlike the $D1$ line. The Landé factor $g_\perp$ along the magnetic moments is not equal to zero in the $D2$ state (see Table 1). Therefore, both the ground and the excited states should take part in the exchange splitting between

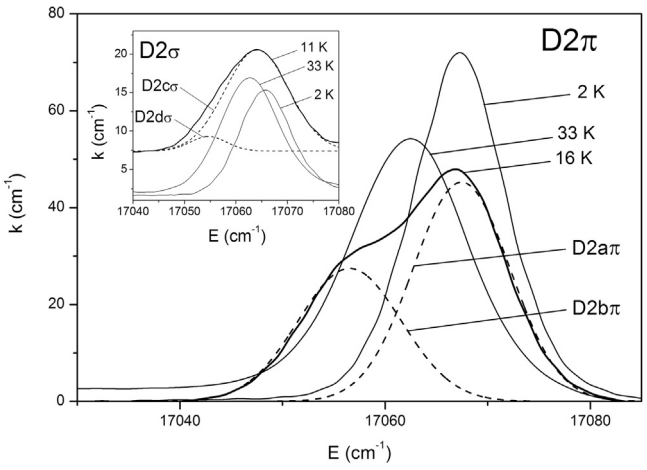

Fig. 9. π-polarized absorption spectra of the $D2$ transitions at several temperatures in zero magnetic field. Inset: the same at σ-polarization.

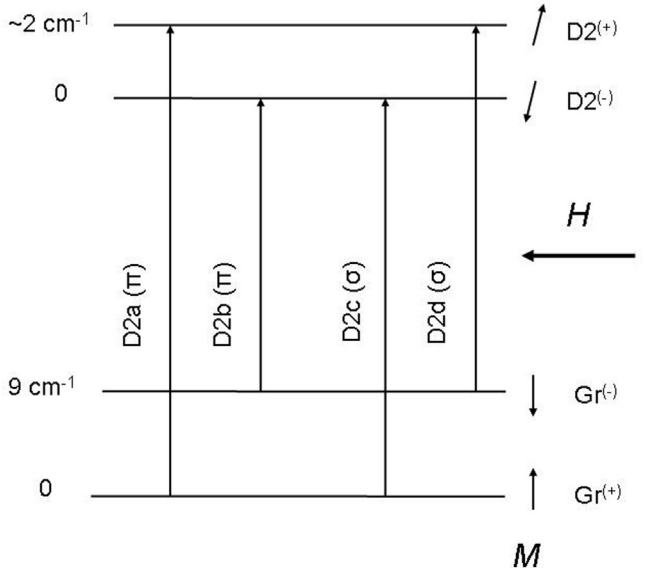

Fig. 10. Diagram of the *D*2 transitions.

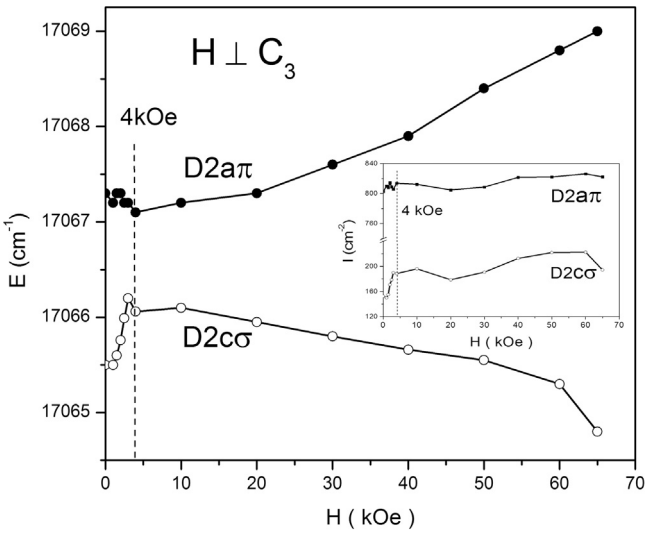

Fig. 12. The *D*2 transitions energies as a function of magnetic field $H \perp C_3$ at $T=2$ K. Inset: the *D*2 transitions intensities as a function of magnetic field $H \perp C_3$ at $T=2$ K.

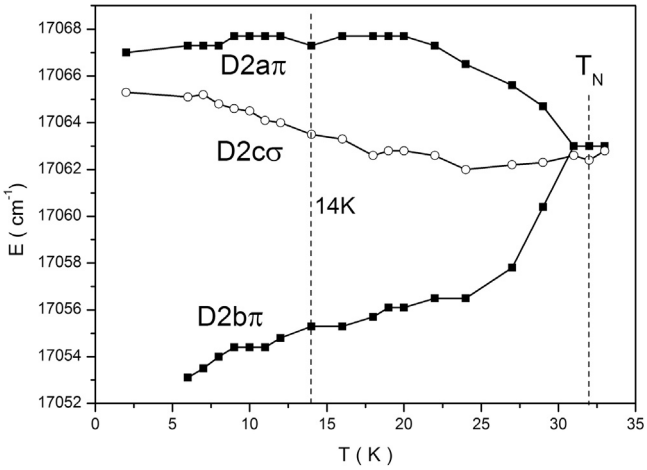

Fig. 11. The *D*2 transitions energies as a function of temperature in zero magnetic field.

*D*2*aπ* and *D*2*bπ* lines. The exchange splitting of the *π*-polarized line, found from Fig. 11 ($\sim$14 cm^{-1} at 6 K), is larger than the found earlier [30] exchange splitting of the ground state ($\sim$9 cm^{-1}), i.e., the exchange splitting of the ground and excited states are summarized. This is possible in the case of the transitions diagram shown in Fig. 10. The sum of the excited state exchange splitting and found earlier splitting of the ground state is not exactly equal to the splitting between *D*2*aπ* and *D*2*bπ* lines. However, it is necessary to note that the ground state exchange splitting found from different transitions is also appreciably different [30].

There are two variants of the transitions diagram from the view-point of the energetically favorable orientation of the sublattice magnetic moment in the excited state. In the first one it is the same as that in the ground state and then the transitions *D*2*a* and *D*2*b* occur with overturn of the magnetic moment direction. In the second variant everything is vice-versa (Fig. 10). We have chosen the second variant, although there is no yet a strong criterion for the choice. In this case, transitions *D*2*c* and *D*2*d* occur with the change of the magnetic moment direction.

At a temperature of the magnetic measurements ($T=2$ K), actually only transitions *D*2*aπ* and *D*2*cσ* (Fig. 10) from the lower component of the ground state exchange splitting are observed (Fig. 9). Variations of positions and intensities of these lines as a function of magnetic field $H \perp C_3$ are presented in Figs. 12 and 12, inset, respectively. As mentioned above, at $H > 4$ kOe there are no domains and the magnetic moments of ions are perpendicular to *σ*-polarization (Fig. 1). Then, from the dependence of the intensity in the field range of 0-4 kOe (Fig. 12, inset) we conclude that, in contrast to the *D*1 transition, the *D*2*cσ* transition is more intensive for $M \perp \sigma$ than for $M \| \sigma$. The behavior of *D*2*aπ* and *D*2*cσ* line positions in magnetic field $H \perp C_3$ (Fig. 12) is qualitatively the same as that of *D*1*aπ* and *D*1*cσ* lines (Fig. 5) and can be explained similarly. In particular, in the region of 0-4 kOe the change of the line energies is due to different energies of different domains in the magnetic field. The same as in the case of the *D*1 line, opposite change of the *D*2*aπ* and *D*2*cσ* transitions energy in the magnetic field H > 4 kOe (Fig. 12) can be accounted for in an assumption that spontaneous sublattice angularity occurs (weak ferromagnetic moment ΔM) in the excited *D*2 state. In the magnetic field parallel to C_3 axis the energies of the considered absorption lines steadily increase. The same as in the case of *D*1 state, this means that the spontaneous sublattice angularity does not occur in this direction.

3.2.3. *D*4 line

The absorption spectrum of the *D*4 transition in σ-polarization at 2 K and $H=0$ is similar to that of the *D*1 line (Fig. 4). The spectrum is decomposed into two components of the Gauss shape, which can be identified as transitions from the lower component of the ground state exchange splitting to the components of the exchange splitting of the excited state (Fig. 13). We supposed that the stronger transition *D*4*aσ* occurs without the overturn of the ion magnetic moment. In this case the energetically favorable orientation of the sublattice magnetic moment in the excited state is the same as in the ground state (Fig. 13). The energies of transitions *D*4*aσ* and *D*4*cσ* change identically in the magnetic field $H > 4$ kOe (Fig. 14). Consequently, in the *D*4 excited state the magnetic moments are oriented purely antiferromagnetically (Fig. 13). The absorption spectrum of the *D*4 line in *π*-polarization is not decomposed into components. The energy of this line in the zero magnetic field coincides within the limit of experimental error with that of the *D*4*aσ* line (Fig. 14). Thus, *π*-polarized *D*4 line can be identified as the *D*4*aπ* line, and the *D*4*c* line is not active in *π*-polarization (Fig. 13). Unlike the *D*1 line, the behavior of the

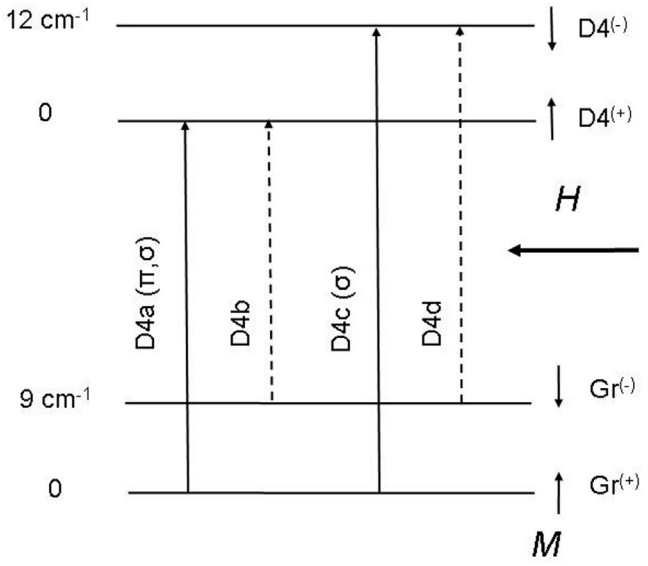

Fig. 13. Diagram of the *D*4 transitions.

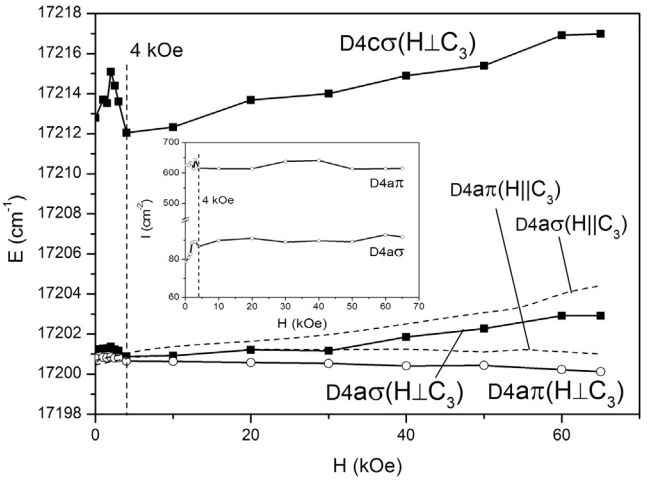

Fig. 14. The *D*4 transitions energies as a function of magnetic field $H\perp C_3$ and $H\|C_3$ at $T=2$ K. Inset: the *D*4 transitions intensities as a function of magnetic field $H\perp C_3$ at $T=2$ K.

*D*4*aπ* and *D*4*aσ* line energies at $H<4$ kOe is similar, but the dependence of the *D*4*aπ* line position on the magnetic field at $H>4$ kOe qualitatively differs from that of the *D*4*aσ* line (Fig. 14). This again looks like the splitting of line (of the *D*4*a* line, in particular) that is not possible for the Kramers doublet. The same as above, this phenomenon can be referred to the absorption in two objects. Indeed, in the noncentro-symmetrical crystal $Nd_{0.5}Gd_{0.5}Fe_3(BO_3)_4$, inversion twins can exist. Additionally, the FeO_6 octahedrons form helicoidal chains, which run parallel to the C_3 axis. The twins and helicoidal chains can be the objects with different optical properties in the magnetic field in the excited D4 state, which correspond to two field dependencies in two polarizations. The positions of *D*4*aσ* and *D*4*aπ* lines in the magnetic field $H\|C_3$ change qualitatively similarly to those in the field $H\perp C_3$ (Fig. 14) i.e., also differently. The magnetic field dependence of the *D*4*aσ* line intensity (Fig. 14, inset) shows that absorption probability for $M\perp\sigma$ prevails in this transition.

The transformation of the *D*4*σ* line with temperature could not be studied because of the influence of the adjacent absorption lines (Figs. 2a and 2b). The absorption spectrum of the *D*4*π* line is not split with the temperature increasing from 2 to 33 K. Consequently, *D*4*b* and *D*4*d* lines (Fig. 13), which could appear with increasing temperature, are not observed, i. e., these transitions are forbidden (at least in π-polarization). The diagrams of *D*4 (Fig. 13) and *D*1 (Fig. 3) transitions are similar to some extent. However, the intensity of the *D*4*cσ* transition is only slightly sensitive to the orientation of the domain magnetic moments relative to *σ*-polarization, while *D*1*cσ* transition is allowed only for $\sigma\|M$. Additionally, there are no indications to the existence of the weak ferromagnetic moment in the *D*4 state.

3.2.4. *D5 line*

At T=2 K, when only the lower ground state sublevel is occupied, the *D*5*π* line is not split (Fig. 15, inset). Consequently, only the transition to one component of the excited state exchange splitting is observed. At higher temperatures the *D*5*π* line is split on two temperature dependent components: *D*5*aπ* and *D*5*bπ* (Fig. 15, inset). Temperature dependence of their positions is depicted in Fig. 15. Splitting of 16.5 cm^{-1} between these lines at 8 K is substantially larger than the exchange splitting of the ground state. Consequently, the exchange splitting of the ground and excited states are summarized and the *D*5 transitions diagram should have the form, shown in Fig. 16. If we suppose that the *D*5*a*

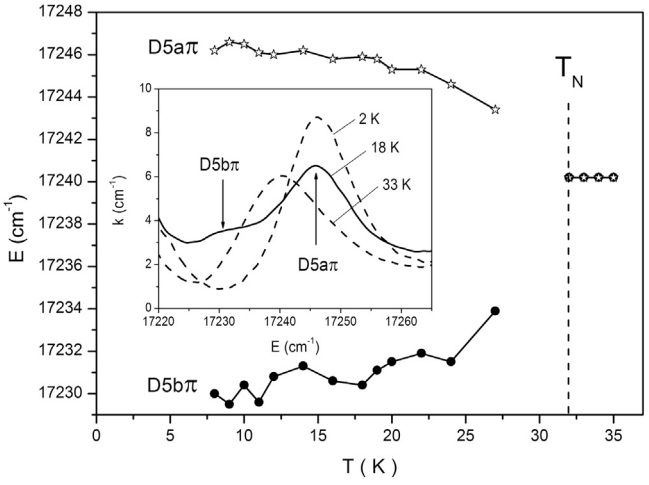

Fig. 15. The *D*5 transitions energies as a function of temperature in zero magnetic field. Inset: *π*- polarized absorption lines at several temperatures.

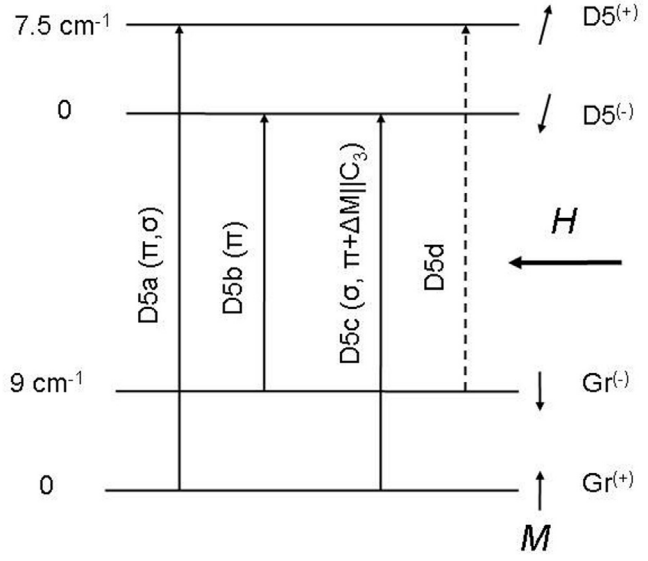

Fig. 16. Diagram of the *D*5 transitions.

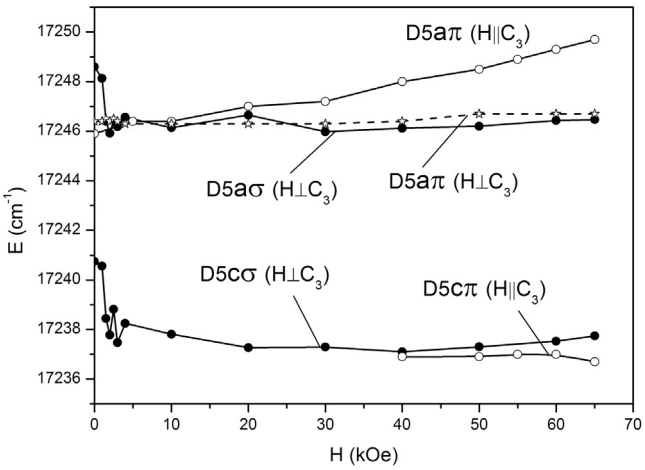

Fig. 17. The *D*5 transitions energies as a function of magnetic field $H\perp C_3$ and $H\parallel C_3$ at $T=2$ K.

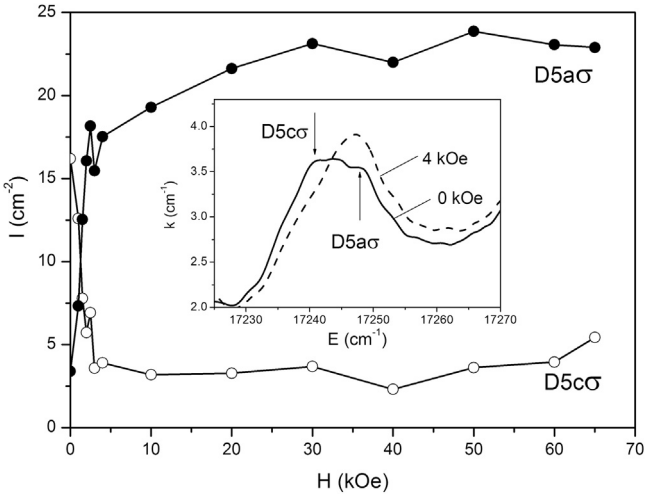

Fig. 18. The *D*5 transitions intensities as a function of magnetic field $H\perp C_3$ at $T=2$ K. Inset: σ-polarized absorption spectra of the *D*5 transition at two magnetic fields.

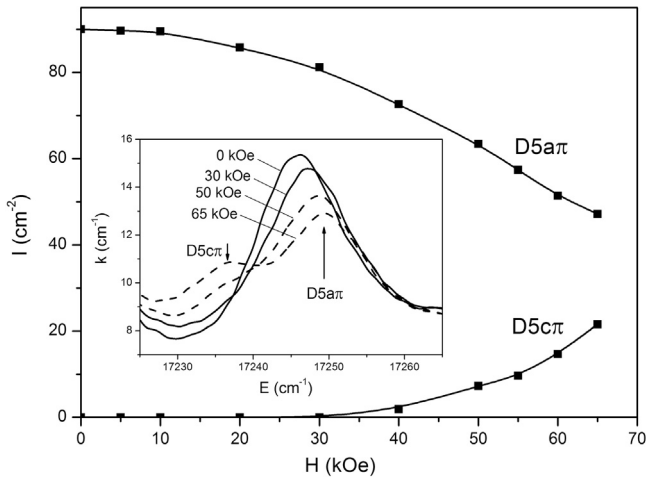

Fig. 19. The *D*5 transitions intensities as a function of magnetic field $H\parallel C_3$ at $T=2$ K. Inset: π-polarized absorption spectra of the *D*5 transition at several magnetic fields.

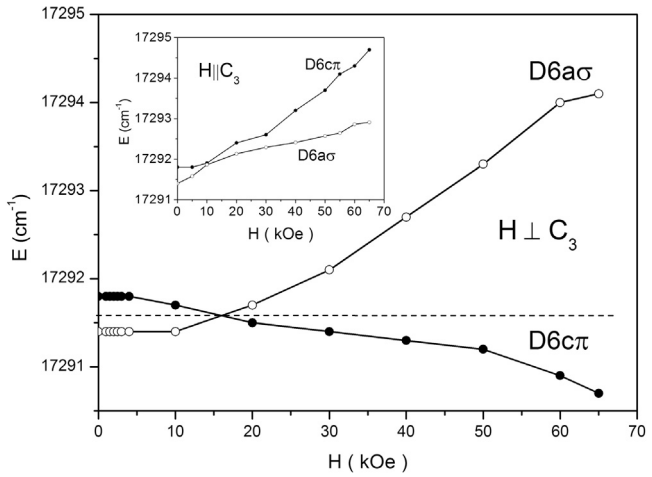

Fig. 20. The *D*6 transitions energies as a function of magnetic field $H\perp C_3$ and $H\parallel C_3$ at $T=2$ K.

transition occurs without the overturn of the ion magnetic moment, then it inevitably follows that the energetically favorable orientation of the ion magnetic moment in the excited state is opposite to that in the ground state (Fig. 16). Position of the *D*5*aπ* line as a function of the magnetic field $H\perp C_3$ at $T=2$ K is shown in Fig. 17.

The *D*5*σ* line at $T=2$ K is decomposed into two components (Fig. 18, inset), which can be identified as *D*5*aσ* and *D*5*cσ* lines (see diagram of Fig. 16). Position of the *D*5*aσ* line as a function of magnetic field $H\perp C_3$ coincides with that of the *D*5*aπ* line at $H>4$ kOe (Fig. 17), but differs from it at $H<4$ kOe. This is the feature already mentioned above in the *D*1 line. The dependences of the *D*5*aσ* and *D*5*cσ* line energies on magnetic field $H\perp C_3$ are parallel within the limit of the experimental error (Fig. 17), i. e. the orientation of the magnetic moments in the *D*5 state are purely antiferromagnetic ones in magnetic field $H\perp C_3$. The intensities of *D*5*aσ* and *D*5*cσ* lines are very sensitive to the orientation of the domains magnetic moments relative to σ-polarization (Fig. 18): the *D*5*aσ* line has mainly $\sigma\perp M$ polarization while the *D*5*cσ* line has mainly $\sigma\parallel M$ polarization, but not purely $\sigma\parallel M$ polarization as it was in the *D*1*c* transition (Fig. 3).

The *D*5 transition reveals peculiar behavior in magnetic field $H\parallel C_3$. The *D*5*π* line is not split in $H\perp C_3$ field. However in the field $H\parallel C_3$ a splitting appears (Fig. 19, inset). From the field dependence of the intensities of the splitting components (Fig. 19) it is seen that a new absorption line appears only at $H>30$ kOe. The line which appeared is identified as *D*5*cπ* line according to its energy (see Fig. 17). The *D*5*aπ* and *D*5*cπ* line energies as a function of $H\parallel C_3$ are also presented in Fig. 17. The opposite direction of these dependences allows us to assume, that the magnetic field $H\parallel C_3$ stimulates the appearance of a weak ferromagnetic moment ΔM, whose direction in $D5^{(-)}$ state coincides with the field direction. The threshold field of the weak ferromagnetic moment inducing is not known exactly since dependence of the *D*5*cπ* line intensity on the ΔM is not known. Therefore $H=30$ kOe of the additional line appearance can be considered only as the approximate threshold field value.

3.2.5. *D6 line*

This absorption line, both in π and σ polarizations, is very nicely approximated by the Lorentz curve and is not split with the increasing temperature and magnetic field. At $T=2$ K there is a small splitting (~ 0.4 cm^{-1}) between π and σ polarized lines. It would be possible to refer this splitting to experimental error, but the field dependences of the lines positions (Fig. 20) show that these are two transitions into the sublevels of the excited state exchange splitting (Fig. 21). Variations of *D*6*aσ* and *D*6*cπ* lines positions in magnetic field $H\perp C_3$ (Fig. 20) show that a weak

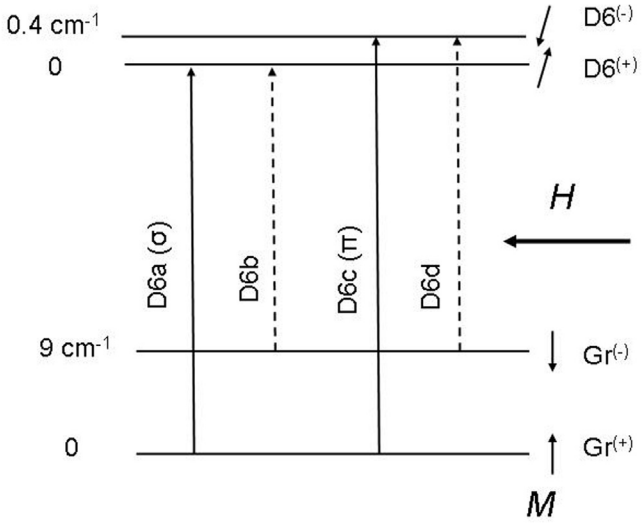

Fig. 21. Diagram of the *D*6 transitions.

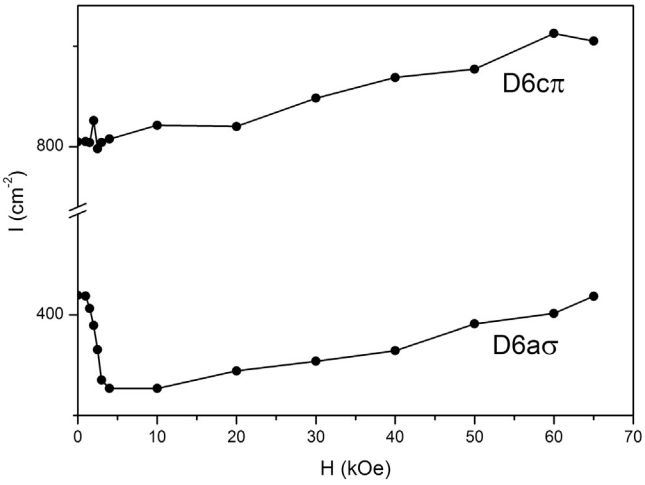

Fig. 22. The *D*6 transitions intensities as a function of magnetic field $H \perp C_3$ at $T=2$ K.

spontaneous ferromagnetic moment appears in the *D*6 excited state. The diagram of Fig. 21 was drawn with this circumstance taken into account. The exchange splitting of the *D*6 state is very small. Therefore the influence of the external magnetic field is relatively large. There is a substantial asymmetry of the field dependencies (Fig. 20) since the external magnetic field also induces the angularity of magnetic moments, but of the same sign in both excited states. Fig. 20, inset testifies that in the magnetic field $H \| C_3$ a weak ferromagnetic moment also exists, but the magnetic states are inverted. The weak ferromagnetic moments, the most probably, are stimulated by the magnetic field. The dependence of the *D*6$a\sigma$ line intensity on the magnetic field $H \perp C_3$ (Fig. 22) shows that polarization $M \| \sigma$ prevails in this absorption.

The excited states *D*3 and *D*7 have the Landé factor $g_\perp = 0$ (see Table 1). Therefore, the splitting of the absorption lines in the exchange field of the iron ordered in the plain $\perp C_3$ should be equal to the exchange splitting of the ground state. However such splitting is not observed. This means that transitions from the upper sublevel of the ground state exchange splitting are forbidden in *D*3 and *D*7 transitions.

3.3. Natural circular dichroism

Natural circular dichroism (NCD) can exist if a crystal structure has no centre of inversion, and NCD was really observed in the studied crystal. The presence of NCD means also that inverse twins of one type prevail. NCD is measured in α-polarized light. NCD spectra of the *D*-band at several temperatures are depicted in Fig. 23. Only *D*1 line demonstrates substantial changes with the temperature decrease and it was studied in detail. The transformation of the NCD spectrum of the *D*1 line with temperature is shown in Fig. 24 and the temperature dependences of the line positions are presented in Fig. 25. The substantial temperature dependent line splitting is observed. For electric dipole transitions

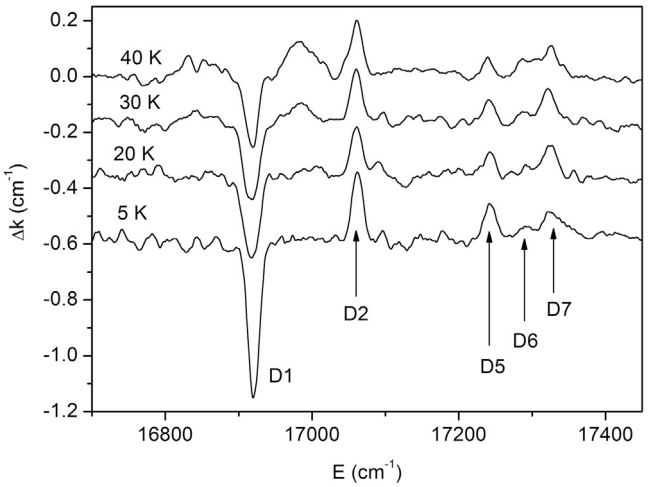

Fig. 23. NCD spectra of the $^4I_{9/2} \rightarrow (^4G_{5/2} + {}^2G_{7/2})$ transition (D-band).

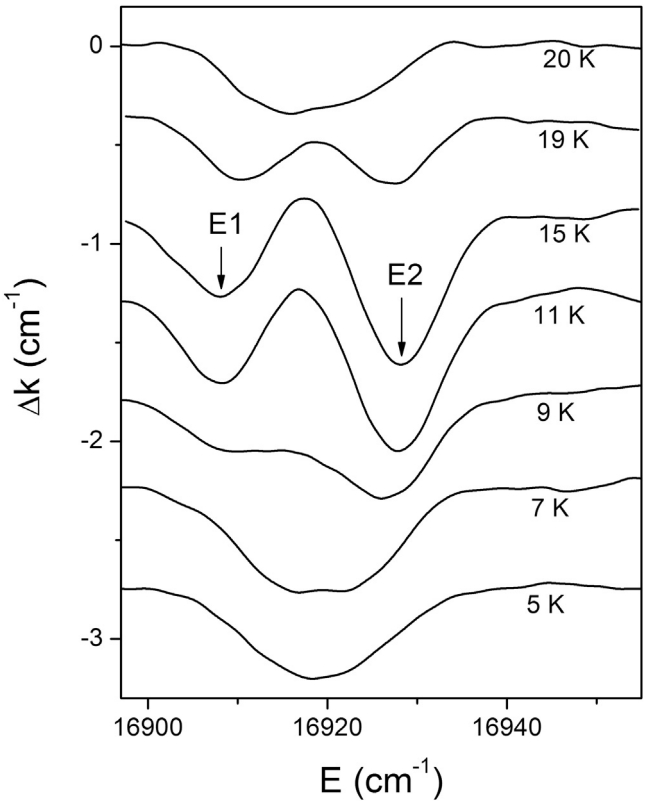

Fig. 24. NCD spectra in the region of the *D*1 line.

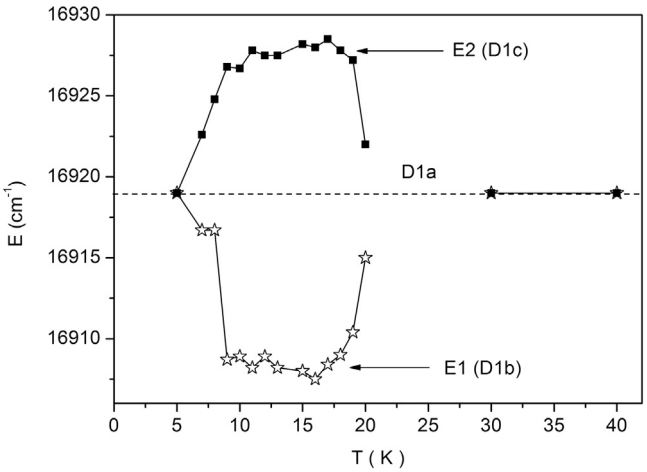

Fig. 25. Energies of components of the NCD spectrum in the region of the *D*1 line as a function of temperature.

α-polarization is equivalent to σ-polarization. However, no any splitting connected with the exchange interaction in the ground state was observed both in σ and π absorption spectra of the *D*1 line (Fig. 7), while an additional temperature dependent absorption line *D*1*b* (Fig. 3) could appear in this case from the low energy side of lines *D*1*a*σ and D1*a*π just at the energy $\sim E1$ of the feature on the NCD spectrum (Fig. 24). According to the above consideration this means that some transitions forbidden in absorption are allowed in NCD.

Natural optical activity (NOA) is defined by the formula:

$$a_N = \frac{R_{if}}{D_{if}} \approx \frac{\langle \Delta k \rangle_0}{\langle k \rangle_0} \tag{3}$$

where k is coefficient of absorption and Δk is NCD. According to [34]:

$$R_{if} = \mathrm{Im}\left[\left\langle i \middle| \vec{d} \middle| f \right\rangle \left\langle f \middle| \vec{m} \middle| i \right\rangle \right] \tag{4}$$

where $\vec{d}$ and $\vec{m}$ are electric and magnetic dipole moments, respectively. $D_{if} = \left| \left\langle i \middle| \vec{d} \middle| f \right\rangle \right|^2$, since considered transitions are mainly of the electric dipole nature. Due to the presence of the magnetic dipole matrix element in (4), selection rules for the NCD can differ from those for electric dipole transitions and other transitions can be allowed in the NCD. In particular, two lines observed in the NCD spectra apparently correspond to *D*1*c* and *D*1*b* transitions (see Fig. 3). Indeed, the energy *E*2 in the region of 10–15 K (Figs. 24 and 25) coincides with the energy of the D1cσ absorption line (Fig. 7). Maximum splitting between *D*1*a* and *D*1*c* lines (Fig. 3) is $\sim 8\ \mathrm{cm}^{-1}$ (Fig. 7) and together with the exchange splitting of the ground state $\sim 9\ \mathrm{cm}^{-1}$ it gives splitting $17\ \mathrm{cm}^{-1}$ between the *D*1*c* and *D*1*b* lines. This value is close to maximum splitting of $\sim 20\ \mathrm{cm}^{-1}$ in the NCD spectrum (Fig. 25). Additionally, sharp decrease of the splitting in the NCD spectrum at 20 K correlates with the disappearance of the *D*1*c*σ transition (Figs. 7 and 8). Fig. 25 allows us to suppose, that at $T=20$ K the *D*1*b* line in NCD also disappears (in absorption it was not observed at all) and only the *D*1*a* line remains. Similar situation takes place at 5 K. Thus, at $T<5$ K and $T>20$ K only the *D*1*a* line remains in the NCD spectrum (Figs. 24 and 25). The *D*1*b* and *D*1*c* transitions have one common feature: they occur with the overturn of the ion magnetic moment (Fig. 3). The disappearance of the *D*1*b* and *D*1*c* lines in NCD at $T=5$ K permits us to infer that at this temperature there are some additional local transformations which are not revealed in the absorption spectra.

4. Summary

Polarized absorption spectra of the $Nd_{0.5}Gd_{0.5}Fe_3(BO_3)_4$ crystal in the region of transition $^4I_{9/2} \rightarrow (^4G_{5/2} + {}^2G_{7/2})$ in Nd^{3+} ion were studied as a function of temperature (2–40 K) and magnetic field (0–65 kOe). The spectra of natural circular dichroism were measured in the range of 5–40 K. The symmetries of Nd^{3+} ion states in the crystal field of D_3 local symmetry were identified in the paramagnetic state of the crystal. In the magnetically ordered state, the splitting of Nd^{3+} ion excited states due to the exchange interaction of Nd^{3+} and Fe^{3+} ions were determined. The investigations in the magnetically ordered state of the $Nd_{0.5}Gd_{0.5}Fe_3(BO_3)_4$ crystal revealed four sets of the new results.

1. The local magnetic properties in the vicinity of the excited ion substantially depend on the excited state. In particular, the values of the Nd^{3+} ion exchange splitting in the excited states are different (Table 1) and in a number of the excited states (*D*1, *D*2 and *D*6) a weak ferromagnetic moment appears (Figs. 3, 10 and 21). In the *D*5 state the weak ferromagnetic moment is stimulated by the external magnetic field in the C_3 direction. In the states *D*2 and *D*5 (Figs. 10 and 16) energetically favorable orientation of the Nd^{3+} ion magnetic moment is opposite to that in the ground state (see also [35]). These observations refer to the more general problem of light induced magnetic phenomena [36].
2. The selection rules for the f-f transitions between components of the exchange splitting of the ground and excited states substantially deviate from those in the paramagnetic state of the crystal. Moreover, they are different for different transitions in spite of the identical symmetry of the studied excited states in the local D_3 symmetry of the crystal in the ground electron state (Table 1). This testifies to the distortions of the local symmetry in the excited states which depend on the excited states. In the spectrum of the natural circular dichroism the transition was revealed that was not observed in the absorption spectrum. This also testifies to the specific selection rules in the magnetically ordered state.
3. The intensities of the transitions substantially depend on the orientation of the sublattice magnetic moment relative to the light polarization, but these dependences are qualitatively different for different transitions. For example, the *D*1*c* transition (Fig. 3) is allowed only in σ-polarization and only when $M \| \sigma$; the *D*5*c* transition (Fig. 16) appears only when the magnetic moment $\Delta M \| C_3$ appears in the magnetic field and so on. It is necessary to remind that in the paramagnetic state all the discussed transitions are allowed both in π and σ polarizations (Table 1).
4. Unexpected result was that in some cases, the energies of the transitions depended on polarization. In particular, in the region 0-4 kOe this occurs in *D*1 and *D*5 transitions (Figs. 5 and 17). At $H>4$ kOe (one domain state) this occurs in *D*4 transition (Fig. 14). It looks like the splitting of the lines that is not possible for the Kramers doublets. Such phenomena can be accounted for by absorption in two objects. In the former case these can be domains and domain walls, in the latter case – inversion twins or helicoidal chains.

It is evident that the magnetic ordering of the crystal is the source of the described peculiar and multifarious properties of selection rules, transitions and electron states. In particular, it is apparently important that the magnetic moments in the studied

crystal are in the plane perpendicular to C_3 axis (Fig. 1). Therefore, they create the second quantization axis besides C_3, and, as a consequence, they create the specific selection rules for the electron transitions, which depend also on the excited states since an electronically excited atom changes the local symmetry and magnetic properties of the crystal. All the states under consideration have $E_{1/2}$ symmetry in D_3 local crystal symmetry (Table 1). However they have different values of J or M_J or both of them (Table 1) and, therefore, the interactions of the atom with the environment are different in these states and the local properties of the crystal are also different.

Acknowledgements

The work was supported by the Russian Foundation for Basic Researches Grant 12-02-00026 and by the President of Russia grant No Nsh-2886.2014.2.

References

[1] W.W. Holloway, E.W. Prohovsky, M. Kestigian, Phys. Rev. 139 A (1965) 954.
[2] A.V. Malakhovskii, I.S. Edelman, Solid State Commun. 28 (1978) 475.
[3] A.V. Malakhovskii, A.L. Sukhachev, S.L. Gnatchenko, I.S. Kachur, V. G. Piryatinskaya, V.L. Temerov, A.S. Krylov, I.S. Edelman, J. Alloys Comp. 476 (2009) 64.
[4] A.V. Malakhovskii, S.L. Gnatchenko, I.S. Kachur, V.G. Piryatinskaya, A. L. Sukhachev, V.L. Temerov, Eur. Phys. J. B 80 (2011) 1.
[5] A.V. Malakhovskii, S.L. Gnatchenko, I.S. Kachur, V.G. Piryatinskaya, A. L. Sukhachev, I.A. Gudim, J. Alloys Compd. 542 (2012) 157.
[6] A.V. Malakhovskii, S.L. Gnatchenko, I.S. Kachur, V.G. Piryatinskaya, A. L. Sukhachev, A.E. Sokolov, A. Ya. Strokova, A.V. Kartashev, V.L. Temerov, Crystallography Reports 58 (2013) 135.
[7] A.V. Malakhovskii, A.L. Sukhachev, A. Yu. Strokova, I.A. Gudim, Phys. Rev. B 88 (2013) 075103.
[8] S. Iwai, J. Phys. Soc. Japan 77 (2008) 113714.
[9] J.J. Longdell, M.J. Sellars, Phys. Rev. A 69 (2004) 032307.
[10] J.H. Wesenberg, K. Mølmer, L. Rippe, S. Kröll, Phys. Rev. A 75 (2007) 012304.
[11] S. Bertaina, S. Gambarelli, A. Tkachuk, I.N. Kurkin, B. Malkin, A. Stepanov, B. Barbara, Nature Nanotechnology 2 (2007) 39.
[12] A.I. Lvovsky, B.C. Sanders, W. Tittel, Nature photonics 3 (2009) 706.
[13] A.K. Zvezdin, S.S. Krotov, A.M. Kadomtseva, G.P. Vorob'ev, Y.F. Popov, A. P. Pyatakov, L.N. Bezmaternykh, E.A. Popova, Pis'ma v ZhETF 81 (2005) 335 ([JETP Lett. 81 (2005) 272]).
[14] A.K. Zvezdin, G.P. Vorob'ev, A.M. Kadomtseva, Yu. F. Popov, A.P. Pyatakov, L. N. Bezmaternykh, A.V. Kuvardin, E.A. Popova, Pis'ma v ZhETF 83 (2006) 600 ([JETP Lett. 83 (2006) 509]).
[15] F. Yen, B. Lorenz, Y.Y. Sun, C.W. Chu, L.N. Bezmaternykh, A.N. Vasiliev, Phys. Rev. B 73 (2006) 054435.
[16] A.M. Kadomtseva, Yu.F. Popov, G.P. Vorob'ev, A.A. Muhin, V.Yu. Ivanov, A. M. Kuzmenko, L.N. Bezmaternykh, Pis'ma v ZhETF 87 (2008) 45 ([JETP Lett. 87 (2008) 39]).
[17] R.P. Chaudhury, F. Yen, B. Lorenz, Y.Y. Sun, L.N. Bezmaternykh, V.L. Temerov, C. W. Chu, Phys. Rev. B 80 (2009) 104424.
[18] A.M. Kadomtseva, Yu. F. Popov, G.P. Vorob'ev, A.A. Mukhin, V. Yu. Ivanov, A.M. Kuz'menko, A.S. Prokhorov, L.N. Bezmaternykh, V.L. Temerov, I.A. Gudim, in Proceedings *of the XXI International Conference "New in Magnetism and Magnetic Materials," Moscow*, 2009, p. 316.
[19] A.V. Malakhovskii, E.V. Eremin, D.A. Velikanov, A.V. Kartashev, A.D. Vasil'ev, I. A. Gudim, Fiz. Tverd, Tela 53 (2011) 1929 ([Phys. Solid State 53 (2011) 2032]).
[20] N. Tristan, R. Klingeler, C. Hess, B. Büchner, E. Popova, I.A. Gudim, L. N. Bezmaternykh, J. Magn. Magn. Mater. 316 (2007) e621.
[21] E.A. Popova, N. Tristan, C. Hess, R. Klingeler, B. Büchner, L.N. Bezmaternykh, V. L. Temerov, A.N. Vasil'ev, JETP 105 (1) (2007) 105.
[22] J.A. Campá, C. Cascales, E. Gutiérrez_Puebla, M.A. Monge, I. Rasines, C. Ruíz-Valero, Chem. Mater. 9 (1997) 237.
[23] M.N. Popova, E.P. Chukalina, T.N. Stanislavchuk, B.Z. Malkin, A.R. Zakirov, E. Antic-Fidancev, E.A. Popova, L.N. Bezmaternykh, V.L. Temerov, Phys. Rev. B 75 (2007) 224435.
[24] P. Fischer, V. Pomjakushin, D. Sheptyakov, L. Keller, M. Janoschek, B. Roessli, J. Schefer, G. Petrakovskii, L. Bezmaternikh, V. Temerov, D. Velikanov, J. Phys.: Condens. Matter 18 (2006) 7975.
[25] M. Janoschek, P. Fischer, J. Schefer, B. Roessli, V. Pomjakushin, M. Meven, V. Petricek, G. Petrakovskii, L. Bezmaternikh, Phys. Rev. B 81 (2010) 094429.
[26] G.A. Zvyagina, K.R. Zhekov, I.V. Bilych, A.A. Zvyagin, I.A. Gudim, V.L. Temerov, Low Temp. Physics 37 (2011) 1269.
[27] J.E. Hamann-Borrero, M. Philipp, O. Kataeva, M. v. Zimmermann, J. Geck, R. Klingeler, A. Vasiliev, L. Bezmaternykh, B. Büchner, C. Hess, Phys. Rev. B. 82 (2010) 094411.
[28] J.E. Hamann-Borrero, S. Partzsch, S. Valencia, C. Mazzoli, J. Herrero-Martin, R. Feyerherm, E. Dudzik, C. Hess, A. Vasiliev, L. Bezmaternykh, B. Büchner, J. Geck, Phys. Rev. Letters 109 (2012) 267202.
[29] A.V. Malakhovskii, A.L. Sukhachev, A.A. Leont'ev, I.A. Gudim, A.S. Krylov, A. S. Aleksandrovsky, J. Alloys Compd. 529 (2012) 38.
[30] A.V. Malakhovskii, S.L. Gnatchenko, I.S. Kachur, V.G. Piryatinskaya, A. L. Sukhachev, I.A. Gudim., J. Alloys Compd. 542 (2012) 157.
[31] A.D. Balaev, L.N. Bezmaternykh, I.A. Gudim, V.L. Temerov, S.G. Ovchinnikov, S. A. Kharlamova, J. Magn. Magn. Mater. 258-259 (2003) 532.
[32] A.L. Sukhachev, A.V. Malakhovskii, I.S. Edelman, V.N. Zabluda, V.L. Temerov, I. Ya. Makievskii, J. Magn. Magn. Mater. 322 (2010) 25.
[33] M.A. El'yashevitch, Spectra of rear earths, Moskow (1953) (in Russian).
[34] W. Moffit, A. Moscovitz, J. Chem. Phys. 30 (1959) 648.
[35] V.V. Eremenko, N.E. Kaner, Yu. G. Litvinenko, V.V. Shapiro, Sov. Phys. JETP 57 (1983) 1312.
[36] V.F. Kovalenko, E.L. Nagaev, Usp. Fiz. Nauk 148 (1986) 561 ([Sov. Phys. Usp. 29 (1986 297)]).